N94-35890

ROBUSTNESS PROPERTIES OF LQG OPTIMIZED COMPENSATORS FOR COLLOCATED RATE SENSORS

A. V. Balakrishnan†

Flight Systems Research Center

University of California at Los Angeles

p 19

Abstract

In this paper we study the robustness with respect to stability of the closed-loop system with collocated rate sensors using LQG (mean square rate) optimized compensators. Our main result is that the transmission zeros of the compensator are precisely the structure modes when the actuator/sensor locations are "pinned" and/or "clamped": i.e., motion in the direction sensed is not allowed. We have stability even under parameter mismatch, except in the unlikely situation where such a mode frequency of the assumed system coincides with an undamped mode frequency of the real system and the corresponding mode shape is an eigenvector of the compensator transfer function matrix at that frequency. For a truncated modal model — such as that of the NASA LaRC Phase Zero Evolutionary model — the transmission zeros of the corresponding compensator transfer function can be interpreted as the structure modes when motion in the directions sensed is prohibited.

1. Introduction

The robustness of control laws to parameter uncertainty is of particular importance to Space applications because testing large structures under the micro-g conditions in Space is not possible on the ground. This paper explores the robustness issue for LQG optimized compensators using the explicit form discovered by the author for their time and/or frequency domain representation, whatever the structure model used — whether it is FEM, Truncated Modal, or Continuum.

The basic properties affecting robustness of the LQG optimized compensator are developed in Section 2 and how they relate to robustness is examined in Section 3. Section 4 deals with continuum models where in particular we show that the transmission zeros are the modes of the structure when the actuator/sensor locations are "pinned" and/or "clamped," i.e., motion in the directions sensed is restricted, generalizing the usual notions for simple beams.

When a truncated modal model is available, the compensator can be expressed explicitly also in terms of the given modes and mode shape vectors. The transmission zeros of these approximate compensators are studied in Section 5 and in particular some numerical results are presented for the NASA LaRC Phase Zero Evolutionary Model. Conclusions are in Section 6.

2. The LQG Optimized Compensator

To state the LQG problem, we begin with the canonical time-domain dynamics of a flexible structure with collocated rate sensors which, whether it is a Finite Element Model or Truncated Modal model (and hence finite dimensional) or a Continuum Model (and hence infinite-dimensional), can be expressed in the form:

$$\left.\begin{aligned} M\ddot{x}(t) + Ax(t) + Bu(t) + BN_a(t) &= 0 \\ v(t) &= B^*\dot{x}(t) + N_r(t) \end{aligned}\right\} \tag{2.1}$$

where in the case of FEM,

M is the mass matrix (nonsingular, nonnegative definite)

A is the stiffness matrix (nonsingular, nonnegative definite)

B is the control matrix (rectangular matrix)

$u(\cdot)$ is the control vector ($n\times 1$, assuming n actuators)

$x(\cdot)$ is the "displacement" vector

$N_a(\cdot)$ is the actuator noise assumed white Gaussian with spectral density $d_a I$, I being the $n\times n$ Identity matrix

$v(\cdot)$ is the sensor output

B^* represents the transpose of B

$N_r(\cdot)$ is the sensor noise assumed white Gaussian with spectral density $d_r I$.

For the Continuum Model such a representation continues to hold, however complicated the structure, with $x(\cdot)$ now allowed to range in a Hilbert space $\mathcal{H}$, with A, M, B being linear operators:

M	bounded linear, self-adjoint, nonnegative definite with M^{-1} bounded;
A	closed linear, self-adjoint, nonnegative definite with compact resolvent, the resolvent set including zero
B	maps E^n Euclidean n-space into $\mathcal{H}$, and
B^*	represents the adjoint of B.

See [1, 2].

The LQG problem we shall consider is that of finding the control $u(\cdot)$ (or equivalently the optimal compensator) that minimizes the mean square time average of the rate:

$$\lim_{T\to\infty} \left\{ \frac{1}{T}\int_0^T \|B^*\dot{x}(t)\|^2\, dt + \frac{\lambda}{T}\int_0^T \|u(t)\|^2\, dt \right\} \tag{2.2}$$

where $\lambda > 0$.

It is shown in [1, 3] that under the "controllability" assumption that

$$B^*\phi_k \neq 0$$

for any k, where ϕ_k are the modes orthonormalized with respect to the mass matrix:

$$A\phi_k = \omega_k^2 M\phi_k\ ; \qquad [M\phi_k, \phi_k] = 1\ , \tag{2.3}$$

the optimal compensator transfer function ($n\times n$ matrix function) can be expressed in the explicit analytical form:

$$\psi(p) = gpB^*(p^2M + A + \gamma pBB^*)^{-1}B\ , \qquad \text{Re. } p \geq 0 \tag{2.4}$$

where

$$g = \frac{\sqrt{d_a/d_r}}{\sqrt{\lambda}}\ ; \qquad \gamma = \sqrt{d_a/d_r} + \frac{1}{\sqrt{\lambda}}\ . \tag{2.5}$$

Moreover, the corresponding mean square control power is given by

$$\lim_{T\to\infty} \frac{1}{T}\int_0^T \|u(t)\|^2\, dt = \frac{d_a}{2\sqrt{\lambda}}\,\text{Tr.}\,(B^*MB)^{-1} \tag{2.6}$$

and the corresponding mean square displacement is:

$$\lim_{T\to\infty} \frac{1}{T}\int_0^T \|B^*x(t)\|^2\, dt = \left(\sqrt{d_a/d_r} + \frac{\sqrt{\lambda}\, d_a}{2}\right)\text{Tr.}\, B^*A^{-1}B\ . \tag{2.7}$$

See [4] for the corresponding time-domain version of (2.4). From (2.3) we can deduce readily that

(i) As $\lambda \to 0$, $g \to \infty$ and $\gamma \to \infty$ we note that $\frac{g}{\gamma} \to \sqrt{d_a/d_r}$ and hence

$$\psi(p) \to I\sqrt{d_a/d_r}$$

where the right side is recognized as is the optimal "static" or "direct connection" or "PID" controller. Note that as $\lambda \to 0$, the control power given by (2.6) becomes infinite, as we expect.

(ii) $\psi(p)$ is "positive real" — that is to say:

$\psi(p)$ holomorphic in $\text{Re.}\, p > 0$

$\psi(p) + \psi(p)^*$ nonsingular, and positive definite, for $\text{Re.}\, p > 0$

where $*$ denotes conjugate transpose. We shall prove this directly, here, even though it may be deduced from the results in [1]. In fact

$$(p^2M + A + \gamma pBB^*)x = 0$$

implies that

$$p^2[Mx, x] + [Ax, x] + \gamma p\|B^*x\|^2 = 0$$

and normalizing so that

$$[Mx, x] = 1$$

we obtain

$$p^2 + \gamma p\|B^*x\|^2 + [Ax, x] = 0 .$$

Because of our assumption that $B^*\phi_k$ is not zero for any k, we see that

$$\|B^*x\| > 0$$

and hence

$$\text{Re.}\, p < 0 .$$

This is enough to imply that in the finite-dimensional case:

$$(p^2M + A + \gamma pBB^*)^{-1}$$

is holomorphic in $\text{Re.}\, p > 0$. In the infinite dimensional case the fact that A has a compact resolvent implies that so does

$$p^2M + A + \gamma pBB^*$$

and hence it follows that

$$B^*(p^2M + A + \gamma pBB^*)^{-1}B$$

is holomorphic in $\text{Re.}\, p > 0$, and in fact is an $\mathcal{H}_\infty$ function.

Next let us calculate

$$\psi(p) + \psi(p)^* , \qquad \text{Re.}\, p \geq 0 .$$

We have

$$\frac{\psi(p) + \psi(p)^*}{2} = B^*(p^2M + A + \gamma pBB^*)^{-1}$$
$$\cdot [|p|^2(p + \bar{p})M + (p + \bar{p})A + 2\gamma|p|^2BB^*](\bar{p}^2M + A + \gamma\bar{p}BB^*)^{-1}B$$

which is ≥ 0, since

$$|p|^2(p + \bar{p})M + (p + \bar{p})A + 2\gamma|p|^2BB^*$$

is, for $\text{Re.}\, p \geq 0$.

In particular for

$$p = i\omega, \qquad -\infty < \omega < \infty$$

we have

$$\frac{\psi(i\omega) + \psi(i\omega)^*}{2} = \gamma\omega^2\psi(i\omega)\psi(i\omega)^*. \tag{2.8}$$

This leads to an important result which we state as:

Lemma 2.1

Suppose for some ω, $-\infty < \omega < \infty$,

$$\text{Re. } [\psi(i\omega)\text{v, v}] = 0 \qquad \text{for some v}. \tag{2.9}$$

Then

$$\psi(i\omega)\text{v} = 0 \tag{2.10}$$

and if $\omega \neq 0$,

$$B^*(-\omega^2M + A)^{-1}B\text{v} = 0. \tag{2.11}$$

Proof.

$$\text{Re. } [\psi(i\omega)\text{v, v}] = \left[\left(\frac{\psi(i\omega) + \psi(i\omega)^*}{2}\right)\text{v, v}\right]$$

which by (2.8) is

$$= \gamma\omega^2\|\psi(i\omega)^*\text{v}\|^2$$

and hence (2.9) is equivalent to:

$$\omega\|\psi(i\omega)^*\text{v}\| = 0.$$

If $\omega = 0$, $\psi(i\omega) = 0$ and hence $\psi(i\omega)\text{v} = 0$.

If ω is not zero,

$$\psi(i\omega)^*\text{v} = 0$$

or

$$B^*(-\omega^2M + A - i\gamma\omega BB^*)^{-1}B\text{v} = 0.$$

Let

$$(-\omega^2M + A - i\gamma\omega BB^*)^{-1}B\text{v} = x$$

or

$$B\text{v} = -\omega^2Mx + Ax - i\gamma\omega BB^*x.$$

Since

$$B^*x = 0,$$

we have

$$Bv = (-\omega^2 M + A)x$$

and ω is not an eigenvalue of A, since $B^*x = 0$. Hence

$$B^*(-\omega^2 M + A)^{-1} Bv = 0.$$

Corollary.
Except for $\omega = 0$, the zeros of

$$\text{Det } |\psi(i\omega) + \psi(i\omega)^*|$$

in $-\infty < \omega < \infty$ are the same as those of

$$\text{Det } |B^*(-\omega^2 M + A)^{-1} B| = 0$$

and in particular independent of g and γ, for $g + \gamma < \infty$.

Proof.

$$\text{Det } |\psi(i\omega) + \psi(i\omega)^*| = 0$$

implies that

$$[(\psi(i\omega) + \psi(i\omega)^*)v, v] = 0, \qquad v \neq 0$$

and hence by the lemma,

$$\psi(i\omega)^* v = 0$$

and since $\omega \neq 0$,

$$B^*(-\omega^2 M + A)^{-1} Bv = 0$$

or,

$$\text{Det } |B^*(-\omega^2 M + A)^{-1} B| = 0.$$

Conversely if

$$\text{Det } |B^*(-\omega^2 M + A)^{-1} B| = 0,$$

so that

$$(B^*(-\omega^2 M + A)^{-1} B)v = 0$$

let

$$(-\omega^2 M + A)^{-1} Bv = x.$$

Then

$$Bv = -\omega^2 Mx + Ax = -\omega^2 Mx + A\gamma \pm \gamma(i\omega) BB^* x$$

for arbitrary value of γ, since $B^*x = 0$. Hence

$$B^*(-\omega^2 M + A \pm \gamma(i\omega) BB^*)^{-1} Bv = 0$$

or

$$(\psi(i\omega) + \psi(i\omega)^*)v = 0$$

or

$$\text{Det } |\psi(i\omega) + \psi(i\omega)^*| = 0 .$$

3. Robustness

The robustness of concern is that with respect to parameter uncertainty, in particular in the mode frequencies ω_k. Thus we want to be able to assert that the closed-loop system is stable even if the parameters chosen for the compensator transfer function $\psi(\cdot)$ are incorrect. Now the closed-loop transfer function corresponding to the compensator transfer function $\psi(\cdot)$ is given by

$$(p^2M + A + \gamma pB\psi(p)B^*)^{-1} . \tag{3.1}$$

Let p be a pole of (3.1), so that for some $x \neq 0$,

$$p^2Mx + Ax + \gamma pB\psi(p)B^*x = 0 . \tag{3.2}$$

Then

$$p^2[Mx, x] + [Ax, x] + \gamma p[B\psi(p)B^*x, x] = 0$$

where $[Mx, x] > 0$.

If $p = 0$, then

$$Ax = 0$$

which is not possible since zero is not an eigenvalue of A — this property of the system is assumed to be known with certainty. If $p \neq 0$, we may divide through by p to get

$$p[Mx, x] + \frac{[Ax, x]}{p} + \gamma[B\psi(p)B^*x, x] = 0 .$$

Let

$$p = \alpha + i\omega , \qquad \alpha \geq 0 .$$

Then

$$\alpha[Mx, x] + \frac{\alpha[Ax, x]}{\alpha^2 + \omega^2} + \gamma[B(\psi(p) + \psi(p)^*)B^*x, x] = 0 . \tag{3.3}$$

Suppose $\alpha > 0$. Then by the positive real property, the third term in (3.3) is positive and the first two terms are of course positive, and hence the sum cannot be zero and hence α cannot be positive. Consider next the case $\alpha = 0$. This yields

$$(i\omega)[Mx, x] - \frac{i[Ax, x]}{\omega} + \gamma[B\psi(i\omega)B^*x, x] = 0 .$$

For this to hold, it is necessary that

$$\text{Re. } [B\psi(i\omega)B^*x, x] = 0$$

where B^*x cannot be zero. Hence, by the lemma

$$\psi(i\omega)B^*x = 0 , \qquad B^*x \neq 0 .$$

But this in turn by (3.2) would imply that

$$\left.\begin{aligned} -\omega^2 Mx + Ax = 0\,; \qquad & B^*x \neq 0 \\ \psi(i\omega)B^*x = 0 \qquad & \end{aligned}\right\} \tag{3.4}$$

In other words an undamped mode-frequency of the system must coincide with a zero of $\psi(i\omega)$ corresponding to the same value of B^*x ("mode shape at the sensor location"). Thus we have robustness with respect to stability so long as this is insured against. Because of the coincidence requirement on the mode shape in addition to the frequency, this is highly unlikely if the controller dimension (number of actuators) is higher than one.

4. Continuum Models

For the case of the continuum model, whether explicit or conceptual, we can relate the zeros of the compensator transfer function to the model in a simple way — viz., we can show that they are the "pinned" and/or "clamped" mode frequencies of the structure or a slight generalization thereof.

We begin with the general case of a multi-beam model as the NASA LaRC Phase Zero Evolutionary Model [5]. Here the state variable $x(\cdot)$ has the form (see [2]):

$$x = \begin{vmatrix} f \\ b \end{vmatrix}$$

where $f(\cdot)$ represents the displacement (6×1) vector and b the corresponding "boundary" values at the nodes, and thus a finite dimensional vector. Also

$$Mx = \begin{vmatrix} M_0 f \\ M_b b \end{vmatrix}$$

$$Ax = \begin{vmatrix} A_0 f \\ A_b f \end{vmatrix} \qquad x \in \mathfrak{D}(A)$$

$$Bu = \begin{vmatrix} 0 \\ B_u u \end{vmatrix} \qquad \text{(where } B_u^* B_u \text{ is nonsingular)}$$

where the dimension of U (the control vector) can be smaller than that of b, and B_u maps U into the finite-dimensional space spanned by b. In this case

$$\text{Det } |B^*(-\omega^2 M + A)^{-1} B| = 0 \tag{4.1}$$

and equivalently, for some v:

$$(-\omega^2 M + A)x = B\text{v}\,; \qquad B^*x = 0\,;$$

which under the notation:

$$x = \begin{vmatrix} f \\ b \end{vmatrix}$$

becomes:

$$-\omega^2 M_0 f + A_0 f = 0 \tag{4.2}$$

$$B_u^* b = 0 \tag{4.3}$$

$$-\omega^2 M_b b + A_b f = B_u v \tag{4.4}$$

The condition (4.4) is superfluous since v is not specified and all we require is that v and hence $B_u v$ be nonzero. Thus the transmission zeros are the eigenvalues of the differential operator A_0 with the "boundary condition" specified by

$$-\omega^2 M_0 f + A_0 f = 0 \; ; \qquad B_u^* b = 0 \; . \tag{4.5}$$

These are recognized as structure modes when the control/sensor locations are "pinned" and/or "clamped" — motion in the directions sensed is not allowed. The structure modes when all nodes are clamped are of course given by:

$$\left.\begin{aligned} -\omega^2 M_0 f + A_0 f = 0 \, , \qquad f \neq 0 \\ b = 0 \, . \end{aligned}\right\} \tag{4.6}$$

If all nodes are control nodes so that B_u is the identity, these are also transmission zeros but not in general because of the additional condition (4.4).

As shown in [3], (4.1) can be further reduced to:

$$|B_u^*(-\omega^2 M_b + T(i\omega))^{-1} B_u| = 0 \tag{4.7}$$

where the "clamped" mode frequencies given by (4.6) are the "poles" of the matrix $T(i\omega)$.

A textbook example of (4.7) is provided by the torsion of a one-dimensional beam with one end clamped and the other end the control node. Here $T(i\omega)$ is given by (see [3] for details):

$$T(i\omega) = \sqrt{\rho G}\, I_\psi \, \omega \cot (2\ell\sqrt{\rho/G}\,)\omega$$

and hence the compensator transmission zeros are given by

$$\sin (2\ell\sqrt{\rho/G}\,)\omega = 0$$

or

$$\omega = \frac{n\pi}{2\ell\sqrt{\rho/G}}$$

whereas the structure undamped modes are given by

$$m\omega = (\sqrt{\rho G}\,) I_\psi \cot (2\ell\sqrt{\rho/G}\,)\omega \, .$$

Note that asymptotically these frequencies merge — a phenomenon which can be proved to hold generally. In this (one-dimensional) case the zeros and poles of

$$(-\omega^2 m + T(i\omega))$$

alternate (an instance of Foster's Theorem familiar in classical circuit analysis [6]) and hence also the compensator transmission zeros and undamped mode frequencies — but this is no longer true in general in the multidimensional case.

5. Truncated Modal Model

Truncated Modal models provide both the (undamped) mode frequencies ω_k and the corresponding mode shapes (column vectors of dimension equal to the control dimension) $B^*\phi_k$ at the sensor locations up to a maximum frequency allegedly adequate for faithful representation of the structure. Assume thus that ω_k, $B^*\phi_k$ are given for $k = 1, \ldots, N$. Then we may consider this the "truth model" and the corresponding optimal compensator transfer function takes the form (see [4]):

$$gpB_N^*(p^2I + D_N + \gamma pB_NB_N^*)^{-1}B_N \tag{5.1}$$

where

$$D_N = \text{Diag.}\ (\omega_1^2, \ldots, \omega_N^2)$$

$$B_N^* = \left| B^*\phi_1 \quad B^*\phi_2 \quad \cdots \quad B^*\phi_N \right|_{n\times N}$$

$$B_N = \left| \begin{matrix} (B^*\phi_1)^* \\ \vdots \\ (B^*\phi_N)^* \end{matrix} \right|_{N\times n}$$

where n is the control dimension (equivalently, the number of actuators). It is assumed that N is large enough so that the $n\times n$ matrix:

$$B_N^*B_N$$

is nonsingular. Then omitting $\omega = 0$, the transmission zeros of the transfer function (5.1) are given by

$$\text{Det}\ |B_N^*(-\omega^2I + D_N)^{-1}B_N| = 0\ . \tag{5.2}$$

For large enough N we should expect these frequencies to closely approximate the structure mode frequencies when motion is restricted along the directions sensed at the actuator/sensor locations. In particular if the theoretical values of the latter are known, we have a means of checking the faithfulness of the truncated model.

For the NASA LaRC Phase Zero Evolutionary Model [5], the truncated modal model has 86 modes. For the corresponding mode shapes as determined by the LaRC team, the frequencies for which (5.2) hold are shown in Figures 1 through 6, where the minimum absolute value of the eigenvalues of

$$B_N^*(-\omega^2I + D_N)^{-1}B_N$$

is plotted as a function of omega for $N = 86$. Note that all the eigenvalues are positive for $\omega < \omega_1$ and negative for $\omega > \omega_N$. Figure 1 shows the entire range from 0-300 radians/second. Figures 2-6 show more detail of the behavior over narrower ranges.

The dependence of zeros on the depth of the modal approximation is illustrated in Figures 7, 8, 9, 1a, 2a, 3a, 4a, 6a and 10a for $N = 8$, 16, 30, corresponding to $\omega_8 = 10.921$, $\omega_{16} = 25.225$, $\omega_{30} = 53.132$, respectively. Note that for the 8-mode model there are no zeros at all, while the 16-mode model shows three zeros (in the range 0-25 rad/sec). The 30-mode model shows excellent agreement with the 86-mode model for ω up to $\omega_{30} = 53.132$, comparing Figures 1 and 1a, 2 and 2a, 3 and 3a, 4 and 4a, 6 and 6a, and finally Figures 10 and 10a show the expected divergence for $\omega > \omega_{30}$. For illustrative purposes we list the first few zeros for the full 86-mode model in rad/sec:

(5.4913)

6.575

8.75

(9.2580)

(14.46)

14.7

(15.26)

where the numbers in parentheses are the nearest undamped mode frequencies.

6. Conclusions

It is shown that the optimal compensator transfer function for LQG rate minimization for flexible structures with collocated rate sensors has transmission zeros at frequencies to the modes of the corresponding continuum structure when the control-sensor locations are "pinned" and/or "clamped" (motion in the directions sensed is curbed). In particular the compensator is robust with respect to stability so long as any such mode of the assumed system does *not* coincide with an undamped mode frequency of the real system and the corresponding mode shape at the sensor locations is an eigenvector of the compensator transfer function matrix at that frequency. For Continuum Models the transmission zeros are shown to be the poles of a matrix function related to the undamped modes. Calculations of the zeros are given for the truncated modal models of the NASA LaRC Phase Zero Evolutionary Model illustrating the dependence on the number of modes used.

References

[1] A. V. Balakrishnan. "Compensator Design for Stability Enhancement with Collocated Controllers," *IEEE Transactions on Automatic Control*, vol. 36, no. 9 (September 1991), pp. 994-1007.

[2] A. V. Balakrishnan. "Modes of Interconnected Lattice Trusses Using Continuum Models, Part 1." NASA CR 189568. December 1991.

[3] A. V. Balakrishnan. "Compensator Design for Stability Enhancement with Collocated Controllers: Explicit Solutions. *IEEE Transactions on Automatic Control*, vol. 37, no. 1 (January 1993).

[4] A. V. Balakrishnan. "An Explicit Solution to the Optimal LQG Problem for Flexible Structures with Collocated Rate Sensors." In: *Proceedings of the 5th NASA-DOD CSI Technology Conference, Lake Tahoe, Nevada, March 3-5, 1992.*

[5] "Langley's CSI Evolutionary Model: Phase Zero." NASA TN 104165. November 1991.

[6] R. W. Newcomb. *Linear Multipart Synthesis*. New York: McGraw-Hill, 1966.

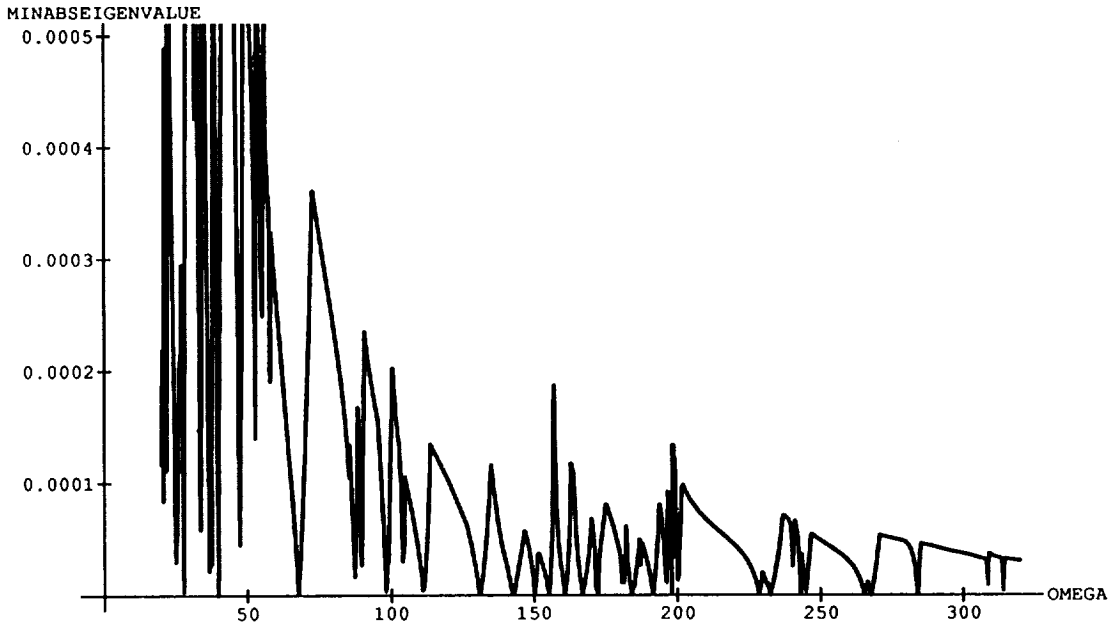

Figure 1

Minimum Absolute Eigenvalue: 86-mode Truth Model

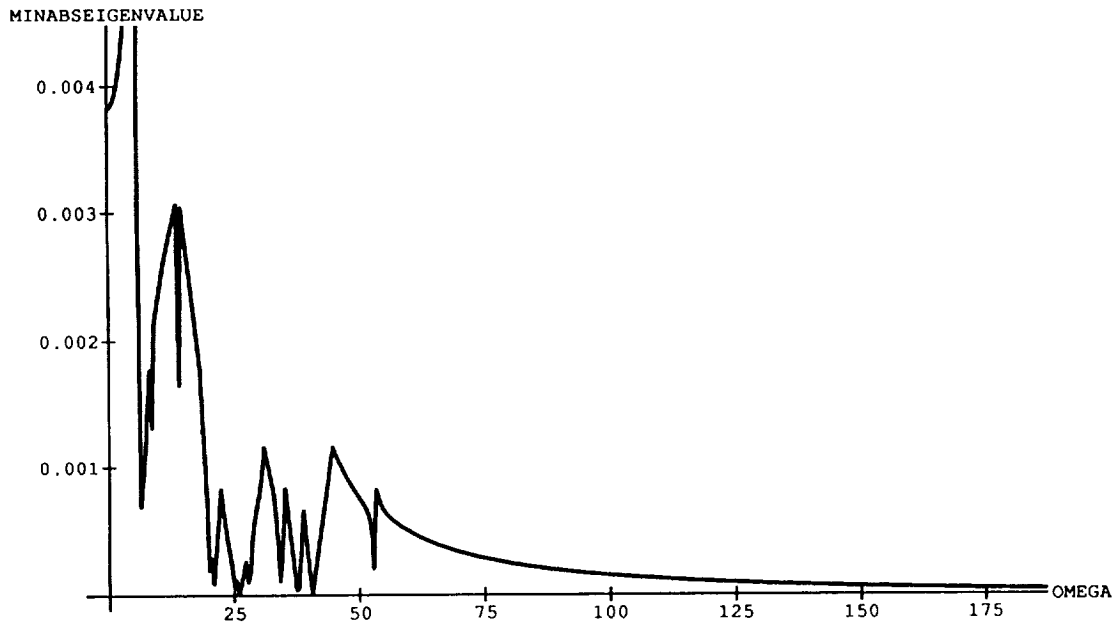

Figure 1a

Minimum Absolute Eigenvalue: 30-mode Truth Model

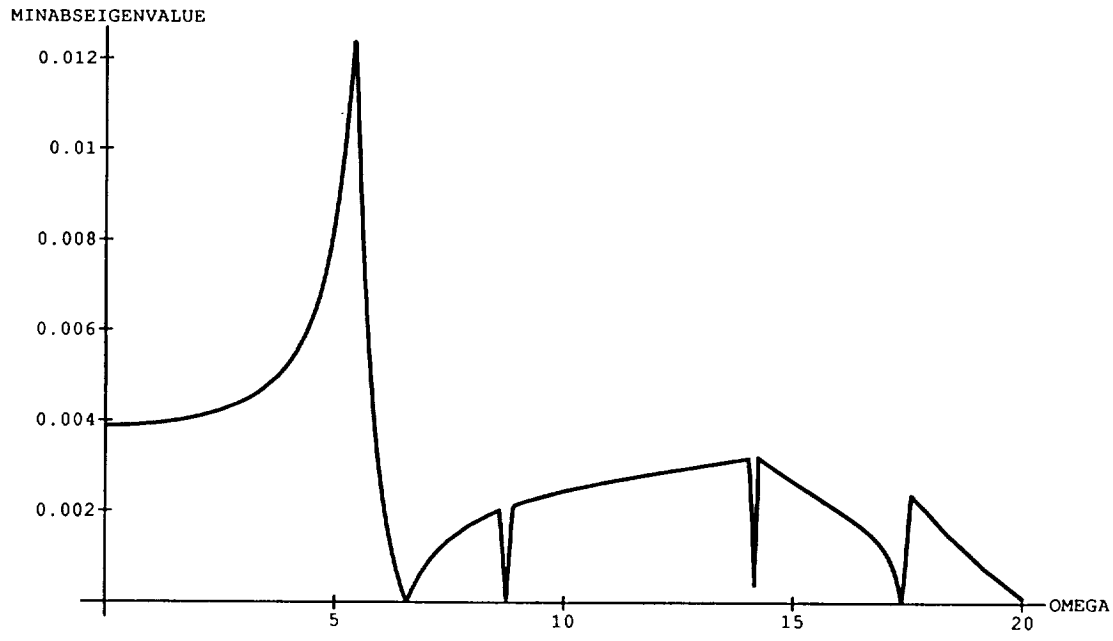

Figure 2

Minimum Absolute Eigenvalue: 86-mode Truth Model

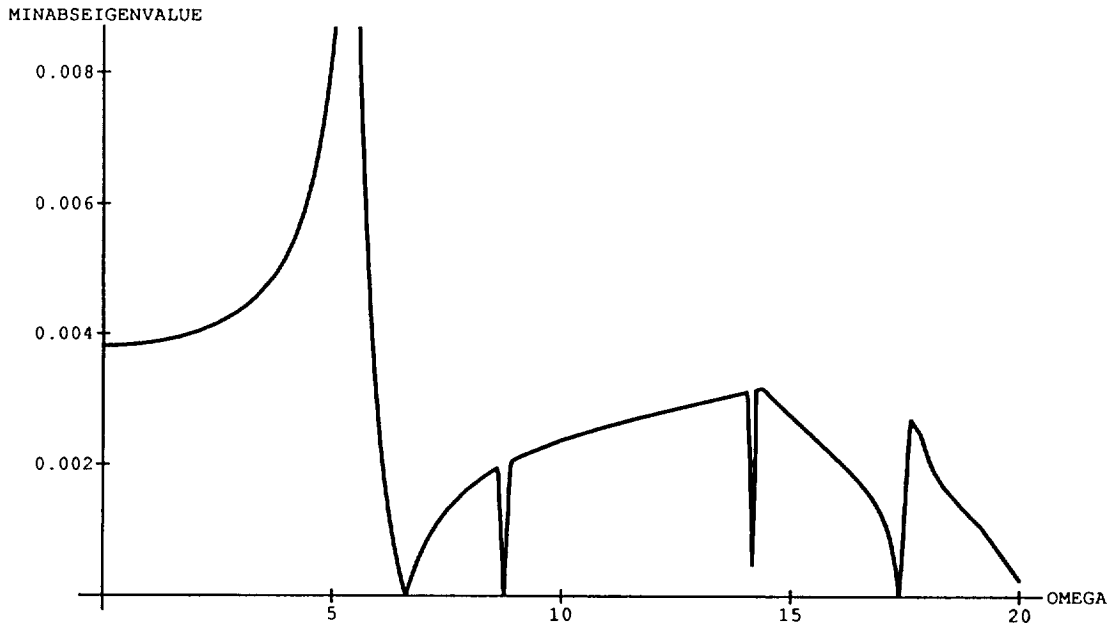

Figure 2a

Minimum Absolute Eigenvalue: 30-mode Truth Model

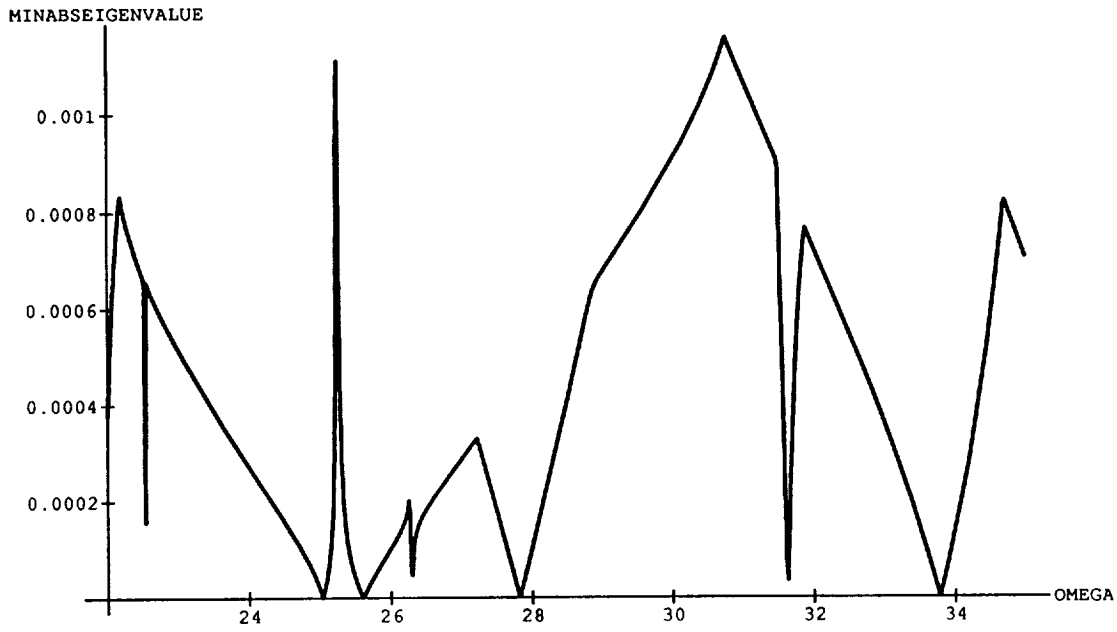

Figure 3

Minimum Absolute Eigenvalue: 86-mode Truth Model

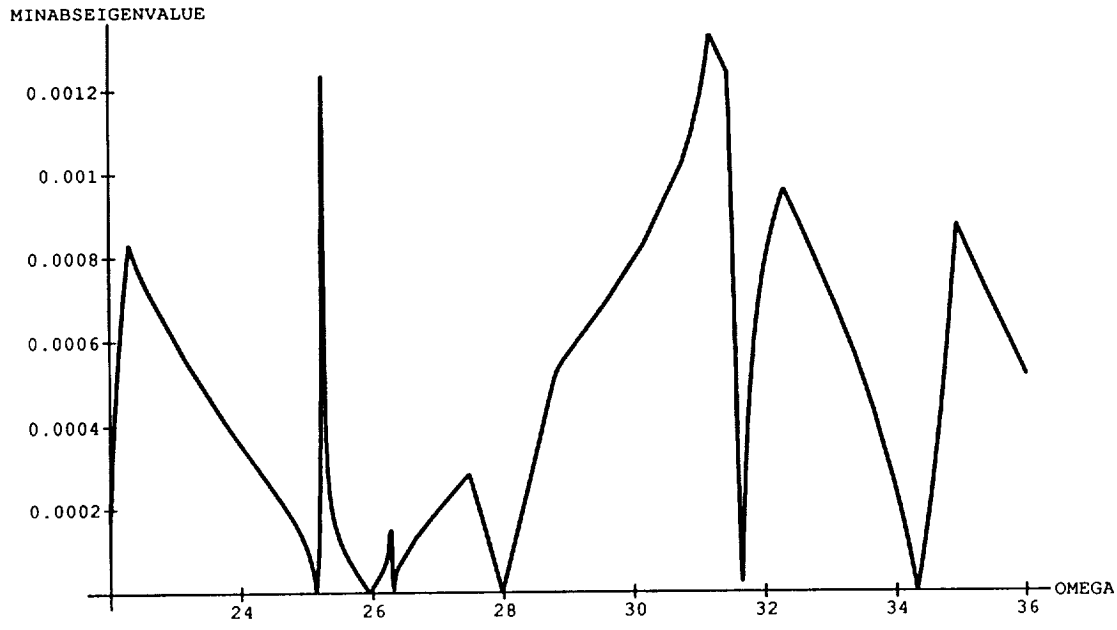

Figure 3a

Minimum Absolute Eigenvalue: 30-mode Truth Model

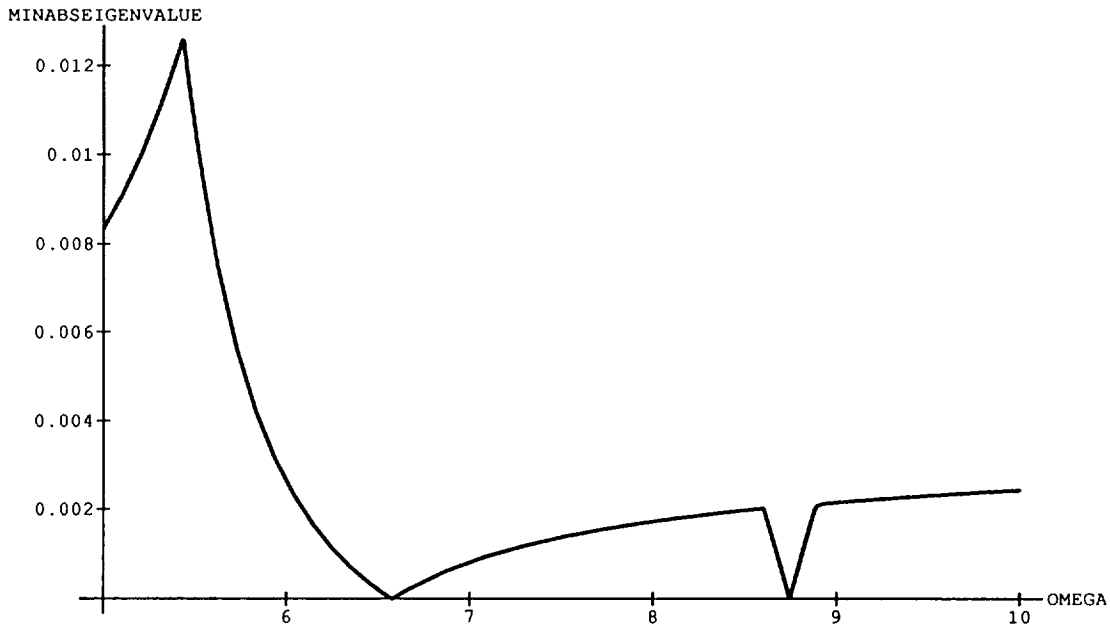

Figure 4

Minimum Absolute Eigenvalue: 86-mode Truth Model

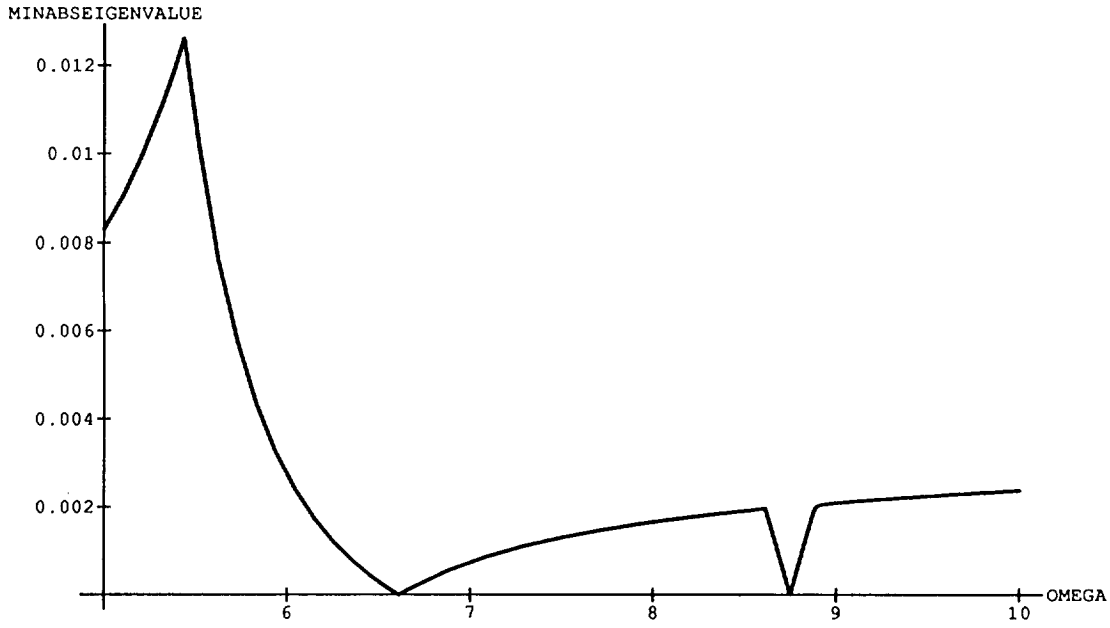

Figure 4a

Minimum Absolute Eigenvalue: 30-mode Truth Model

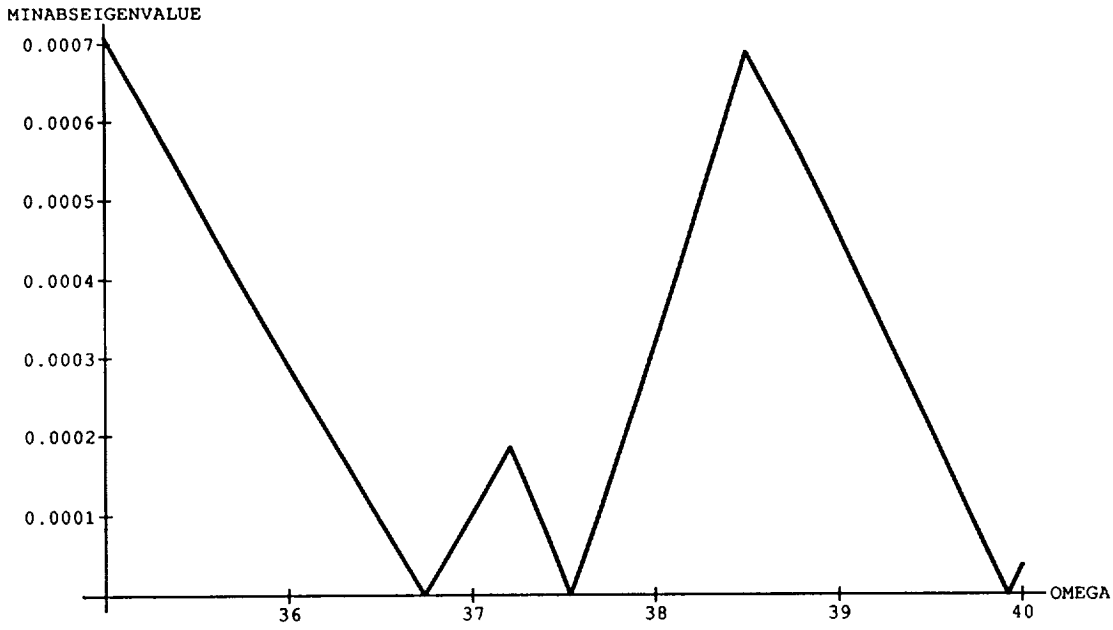

Figure 5

Minimum Absolute Eigenvalue: 86-mode Truth Model

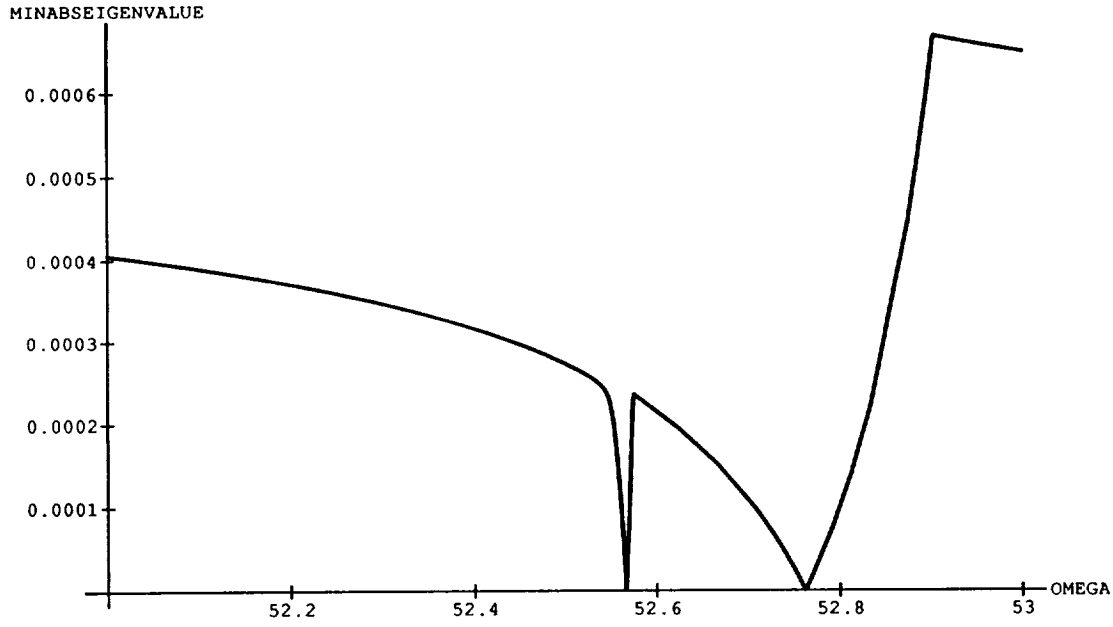

Figure 6

Minimum Absolute Eigenvalue: 86-mode Truth Model

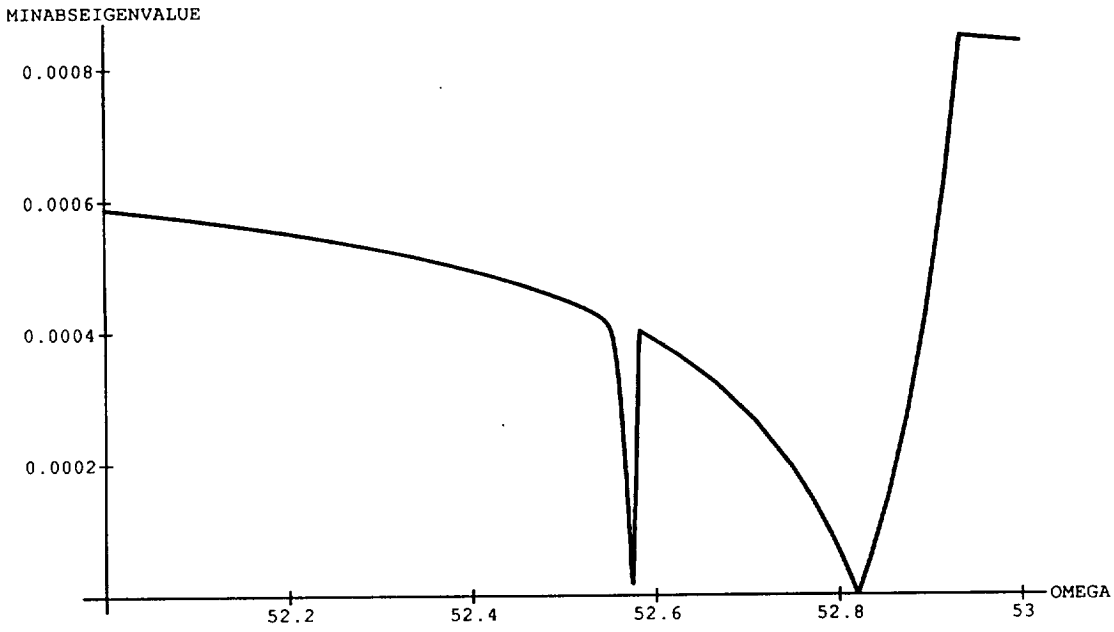

Figure 6a

Minimum Absolute Eigenvalue: 30-mode Truth Model

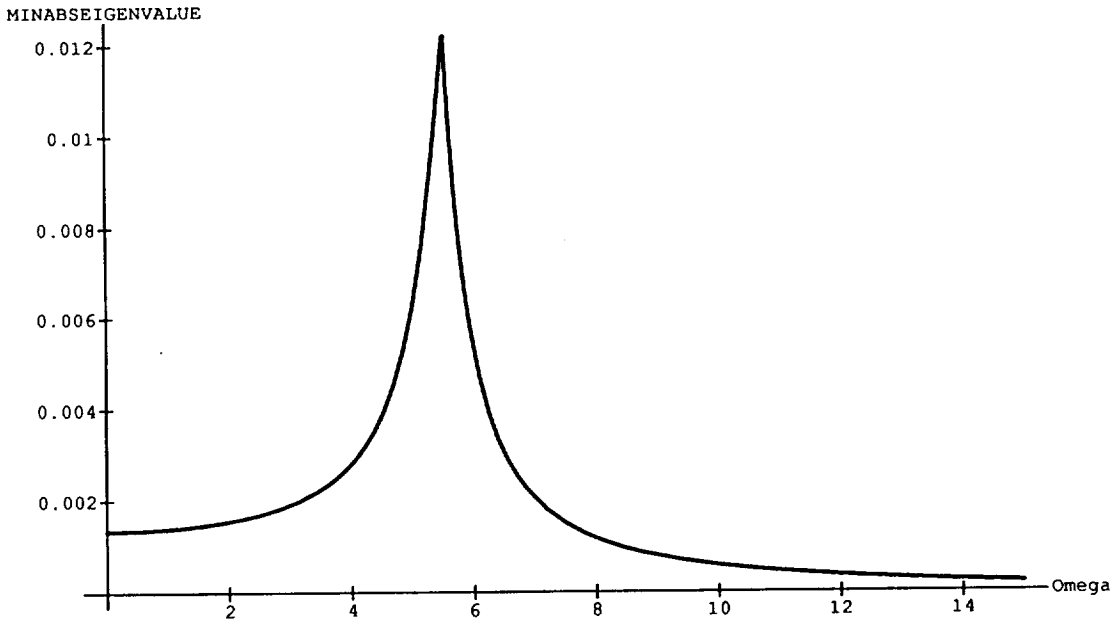

Figure 7

Minimum Absolute Eigenvalue: 8-mode Truth Model

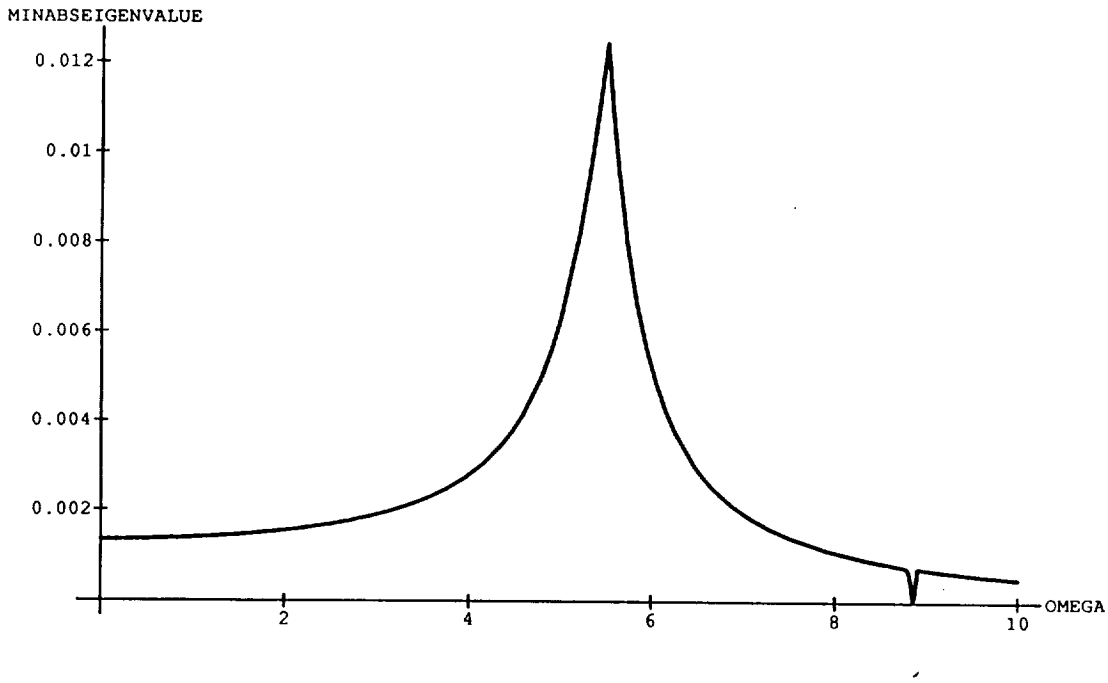

Figure 8

Minimum Absolute Eigenvalue: 16-mode Truth Model

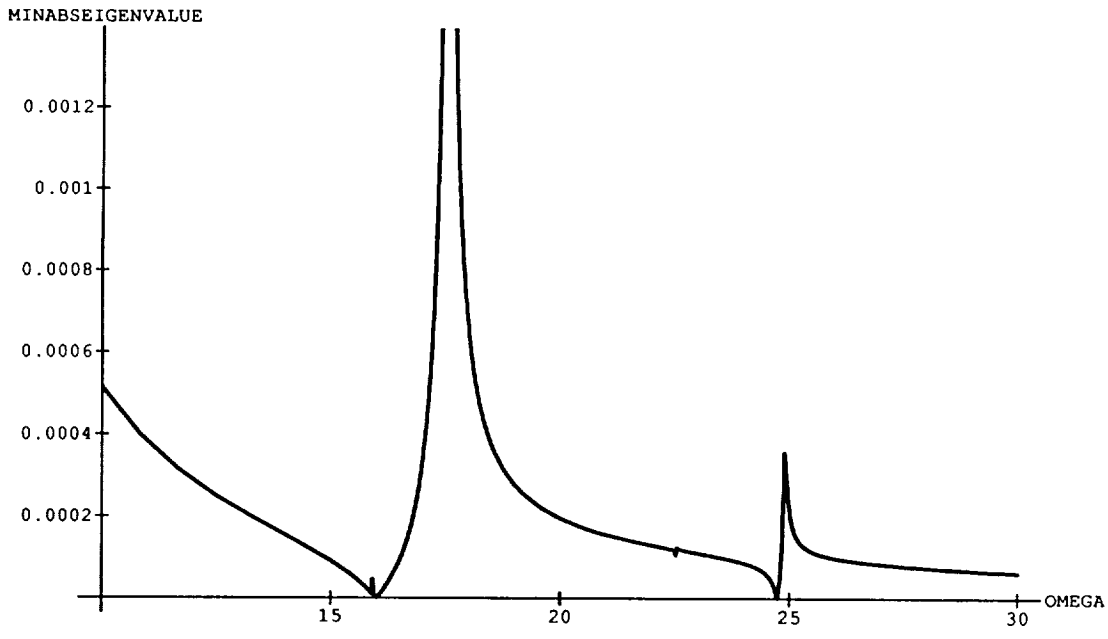

Figure 9

Minimum Absolute Eigenvalue: 16-mode Truth Model

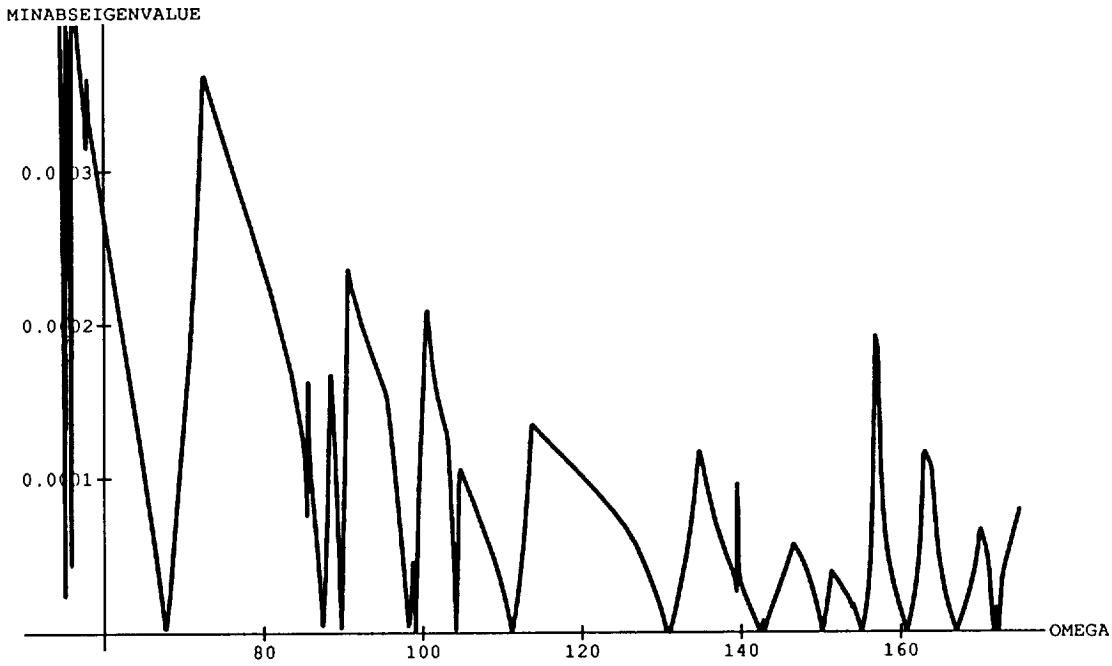

Figure 10

Minimum Absolute Eigenvalue: 86-mode Truth Model

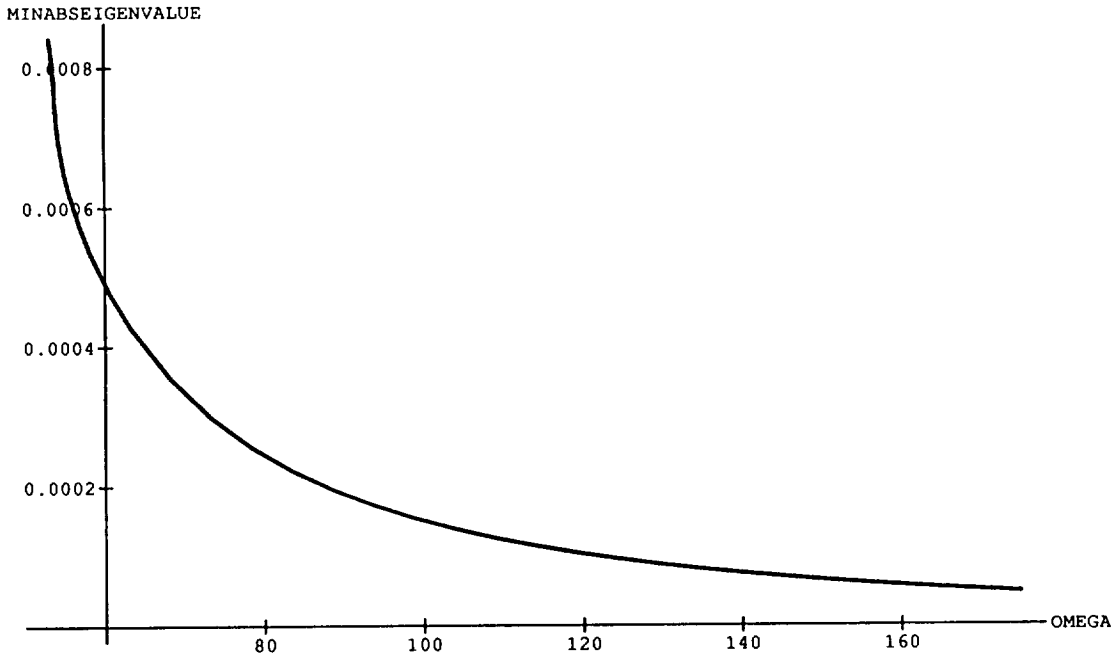

Figure 10a

Minimum Absolute Eigenvalue: 30-mode Truth Model